



HAL
open science

Short range optical communication with GaN-on-Si microLED and microPD matrices

Patrick Le Maitre, Anthony Cibie, Fabian Rol, Stephanie Jacob, Nicolas Michit, Sultan El Badaoui, Bastien Miralles, Julia Simon, Clement Ballot, Bernard Aventurier, et al.

► To cite this version:

Patrick Le Maitre, Anthony Cibie, Fabian Rol, Stephanie Jacob, Nicolas Michit, et al.. Short range optical communication with GaN-on-Si microLED and microPD matrices. Journal of the Society for Information Display, 2024, SPECIAL SECTION PAPER, pp.1-18. 10.1002/jsid.2012 . cea-04768418

HAL Id: cea-04768418

<https://cea.hal.science/cea-04768418v1>

Submitted on 6 Nov 2024


HAL is a multi-disciplinary open access archive for the deposit and dissemination of scientific research documents, whether they are published or not. The documents may come from teaching and research institutions in France or abroad, or from public or private research centers.

L'archive ouverte pluridisciplinaire **HAL**, est destinée au dépôt et à la diffusion de documents scientifiques de niveau recherche, publiés ou non, émanant des établissements d'enseignement et de recherche français ou étrangers, des laboratoires publics ou privés.



Distributed under a Creative Commons Attribution - NonCommercial - NoDerivatives 4.0
International License

Short range optical communication with GaN-on-Si microLED and microPD matrices

Patrick Le Maitre  | Anthony Cibié | Fabian Rol | Stéphanie Jacob |
Nicolas Michit | Sultan El Badaoui | Julia Simon | Bastien Miralles |
Clément Ballot | Bernard Aventurier | Paolo De Martino, SID Member

CEA LETI, Minatec, Univ. Grenoble Alpes, Grenoble Cedex 9, France

Correspondence

Patrick Le Maitre, Univ. Grenoble Alpes, CEA LETI, Minatec, 17 rue des Martyrs, F-38054 Grenoble Cedex 9, France.
Email: patrick.lemaitre@cea.fr

Funding information

IPCEI Microelectronics and Connectivity; Institut Carnot CEA-LETI; French Public Authorities

Abstract

(In)GaN microLEDs have reached a high degree of maturity due to their development in the lighting industry. Their robustness and high efficiency make them ideal candidates for high-brightness, high-resolution micro-displays. Beyond display applications, microLEDs are being explored for non-display uses, including wireless Visible Light Communication (VLC) and parallel communication via multicore fiber. This study investigates short-range chip-to-chip optical communication using InGaN/GaN microLEDs and micro Photodiodes (microPDs). Leveraging processes developed for micro-displays, we address the challenges of integrating GaN microLEDs and microPDs on ASICs. We outline the main figures of merit, including expected energy efficiency, optical coupling to multicore fibers or waveguides, and the spectral efficiency of InGaN/GaN microPDs correlated with TCAD simulation and experimental transmission results. Our study highlights the potential of GaN microLEDs and microPDs for massively parallel, energy-efficient data transmission, paving the way for innovative short-range and energy-efficient optical communication solutions.

KEYWORDS

characterization, communication FDTD, GaN, microLED, microPD, TCAD, VLC

1 | INTRODUCTION

Since the lighting revolution began after the successful industrialization of blue LED, considerable progress has been made over the past 10 years to scale down GaN pixels while mitigating the efficiency loss,¹ making their availability for the industrial display market imminent. While being intensively studied for display applications,

GaN microLEDs, due to their unique brightness characteristic, are also considered for various non-display applications² such as wireless Visible Light Communication (VLC), as reviewed by.³ Furthermore, the idea of using microLEDs for parallel communication through a multicore fiber was explored 15 years ago.^{4,5} Now, with advancements in microLED fabrication techniques originally developed for the display industry, commercial

This is an open access article under the terms of the [Creative Commons Attribution-NonCommercial-NoDerivs](https://creativecommons.org/licenses/by-nc-nd/4.0/) License, which permits use and distribution in any medium, provided the original work is properly cited, the use is non-commercial and no modifications or adaptations are made.

© 2024 The Author(s). *Journal of the Society for Information Display* published by Wiley Periodicals LLC on behalf of Society for Information Display.

applications of these methods are actively being pursued.^{6,7} GaN microLEDs have also been explored as a high-speed photodetector^{8–11} or as a full duplex device combining emitter and receptor functionalities.^{11–14} Although the RF bandwidth of GaN microLED devices is relatively small compared to photonics devices used in near-IR optical communication, their ability to be scaled down to a very low pitch, between 1 μm and 10 μm , their high luminosity and their ability to operate at high temperature make them interesting devices for short-range optical communication. Applications such as artificial intelligence (AI) or high-performance computing (HPC) are pushing forward the development of higher performances, better energy efficiency, and low latency short-range interconnects. Indeed, as reported in,¹⁵ hardware performance required for AI development is scaling much faster than the interconnect and memory data rates. As a consequence, inter- or intra-chip communication is expected to become the main limiting factor in the advancement of AI technology, which strengthens the interest in new short-range optical interconnects such as GaN microLEDs.

We address recent work conducted at CEA-LETI focused on developing short-range chip-to-chip optical communications, as illustrated in Figure 1, using InGaN/GaN microLEDs and micro Photodiodes (microPDs). This work leverages epitaxy, device, and integration processes originally developed for micro-displays and adapted for 200 mm ASICs. After outlining the expected advantages of microLEDs for communication and comparing them to alternative technologies, we will briefly introduce an integration process developed to assemble a dense matrix of microLEDs above a controlling ASIC. The main figures of merit will be highlighted to assess

the overall link performance. The coupling of microLEDs to waveguides or optical fibers will be discussed, based on FDTD simulation results. Additionally, we will examine the performance of InGaN/GaN microPDs based on TCAD simulation results correlated with experimental measurements. Finally, experimental results obtained in transmission and reception using a 200 mm GaN microLED process compatible with ASIC integration will be presented, along with future perspectives.

2 | CHIP-TO-CHIP COMMUNICATION

2.1 | Technologies for short-range communication

Several technologies can be considered for high-speed and energy-efficient short-range interconnects. Silicon photonics is a good candidate. It is energy-efficient when transmitting a huge amount of data through a serial link. Data rates over 100 GB/s per link have been demonstrated.¹⁶ However, it requires the heterogeneous integration of analog, high-speed digital, RF, laser, and photonic IC. Optical communication through VCSEL (Vertical-cavity surface-emitting lasers) is another promising candidate, with full link transmission up to 40 Gb/s at 3.4 pJ/bit reported.¹⁷ Both technologies require data Serialization/Deserialization (SerDes), which takes a substantial circuit area and contributes to half of the power budget in a 2 pJ/bit photonic link.¹⁸

Matrix of microLEDs is an alternative way to achieve data transmission at a short range. Instead of creating a high-speed optical serial link, parallel communication between a matrix of microLEDs and a matrix of microPDs is proposed. In such integration, each microLED transmits a digital signal at a lower data rate than a serial link, presently targeted at 1 Gb/s. The aggregated data rate is proportional to the number of pixels, which makes it theoretically possible to achieve a high level of data rate density (data rate per surface area of emitting area) up to 20 Tb/s/mm² with microLEDs at a pitch of 8 μm . MicroLEDs and microPDs are built directly over a CMOS ASIC by processing 200 mm GaN-on-Si Silicon wafer reported on ASIC. In order to enable emission and reception on the same chip, GaN microPDs, and GaN microLEDs should be made from the same epitaxial GaN wafer. An alternative system would be to have emission and reception separated, which would make it possible to optimize epitaxy separately for each device. MicroLED driver that converts digital signals into current excursions and a Trans-Impedance Amplifier (TIA), that converts small photocurrent into digital voltage, must be placed underneath each

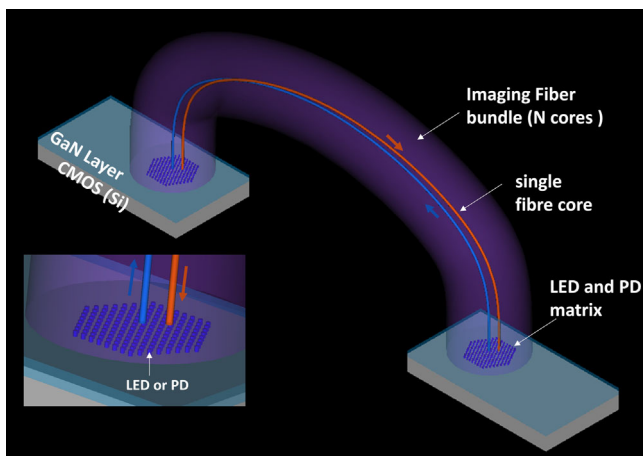


FIGURE 1 Communication system composed of two matrices of GaN microLED and microPDs over ASIC linked via an imaging fiber bundle.

microLED in the CMOS ASIC (Figure 2). MicroLEDs are biased at a constant voltage value, and a current excursion is applied. MicroPDs are biased in reverse voltage.

Communication using microLEDs may offer a good solution for chip-to-chip communication across various system integrations: at chip-scale, between two chips on an interposer, between chips on a single board, or across different boards. Figure 3 shows a non-exhaustive list of system considerations for which microLED communication may be considered. For ultra-short-reach interconnects (in the millimeter range), communication between a microLED and a photodiode could be done through an on-chip waveguide optimized for visible light transmission. This requires optimization of the LED structure to enhance lateral emission. As the communication link distance increases slightly, such as between chiplets in a large interposer, vertical coupling between the microLED and an optical interposer may be considered.

For medium-reach (cm to m), multicore fibers may be used to transmit optical signals from the emitter to the receiver. Fiber bundles, originally developed for endoscopy applications, could enable a very high density of communication channels to transmit light between matrices of microLEDs and microPDs, as described in Figures 1 and 2. Such fibers, for example, the Sumita leached image bundle (ref 126F0910–7.4), can contain up to 16,000 cores of 4.4 μm diameter at a pitch of 7.4 μm over a 1 mm^2 surface, arranged in a hexagonal pattern. Achieving such high data rate density presents a challenge in the packaging of the fiber above the microLED or microPD matrix. It requires precise alignment of the fiber core directly and a spacing of 1–10 μm between the microLED and the fiber end to prevent crosstalk. Considering a solution that eases fiber alignment constraints while slightly reducing the data rate density target may be a viable tradeoff. Utilizing leached imaging

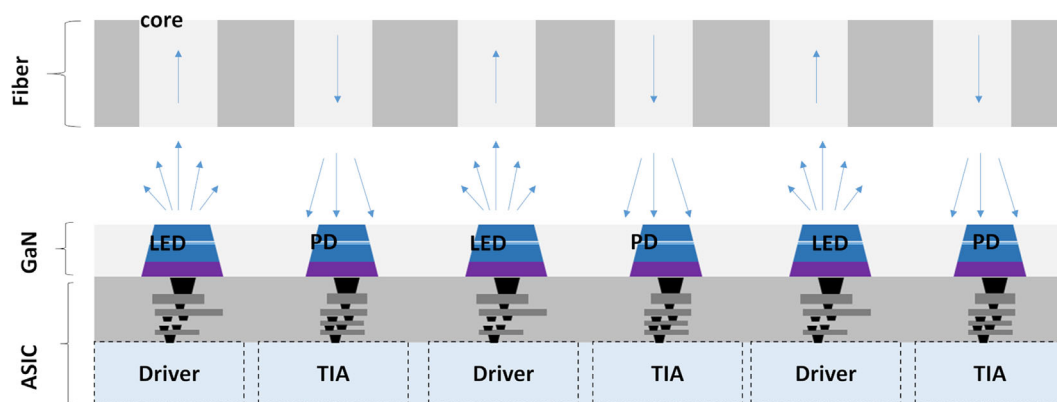


FIGURE 2 Chip-to-chip communication, with CMOS driving and receiving circuit.

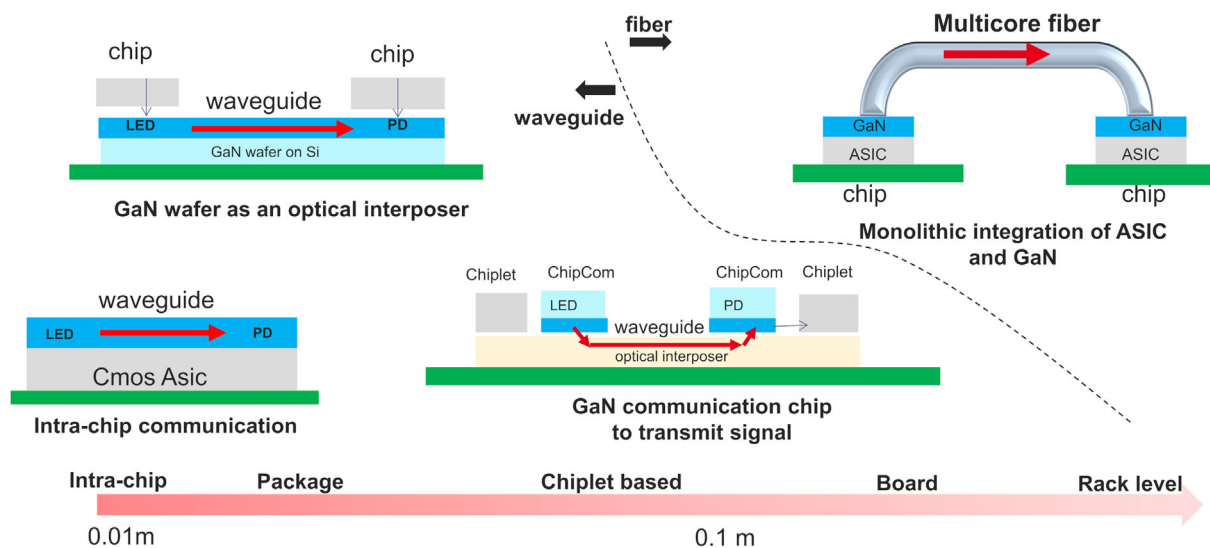


FIGURE 3 Example of system integration that may be considered for chip-to-chip communication with microLED and microPD.

fiber for optical communication has limitations regarding the communication length; to our knowledge, such fibers are not currently produced for distances exceeding 1 to 2 m. Additionally, spectral dispersion is expected over longer distances.

3 | 200 MM FABRICATION PROCESS OF GAN MICROLED AND MICROPD

Achieving high data rate densities, above 10 Tb/mm², requires integrating a matrix of microLEDs and microPDs along with their drivers and TIAs in a very dense way, at pitches under 10 μm, assuming a data rate of 1 Gbps per microLED. Therefore, building microLEDs and microPDs directly above an ASIC is highly desirable for achieving a high density of emitters and receptors. However, directly growing GaN on a CMOS ASIC is not feasible due to thermal constraints. Consequently, several approaches have been considered for the monolithic integration of GaN microLEDs with an ASIC. One approach involves the hybridization of a GaN chip with a CMOS ASIC. To achieve high densities of microLEDs, traditional packaging techniques such as bump flip-chip technology are impractical. Hybridization using microtube technology has been successfully developed in the past, enabling the fabrication of 10 μm pitch microdisplays.¹⁹ Several actors have developed technologies that involve the micro-transfer of individual microLEDs for displays²⁰ and micro-transfer technology was recently employed to create GaN on ASIC microLED demonstrators with a 50 μm pitch for optical communication.⁷ Lastly, hybrid bonding of Sapphire GaN wafers above a 300 mm CMOS

ASIC wafer has been demonstrated,²¹ enabling the fabrication of a 3 μm pixel pitch microdisplay. An alternative approach to hybridization presented in this work consists in realizing GaN epitaxial wafer bonding before pixel definition.

Leveraging technology originally developed for microdisplay applications,²² a process illustrated in Figures 4 and 5 has been developed to integrate a GaN microLED matrix onto a CMOS ASIC specifically to study optical communication applications. Unlike hybrid bonding, the process outlined does not necessitate precise alignment between the ASIC and GaN wafers and makes it possible to realize a very dense matrix at a pitch of 2.5 μm. Initially, an LED epitaxial wafer is transferred onto a conventional Si 100 substrate, which may serve as the ASIC in the final integration, using non-aligned metal–metal bonding. Subsequently, LED mesas are etched to define the emissive areas. Following this, a dielectric passivation layer is deposited to minimize dangling bonds and associated non-radiative recombination. An aluminum mirror is then deposited around the microLEDs to enhance light efficiency. After planarization, openings are created for n-GaN and p-GaN contacts, which are then covered with 300 nm of aluminum to define metal routing and test pads. In this integration approach, the GaN features nitrogen polarity facing upwards, a configuration that is reversed compared to conventional integrations.

The experimental measurements presented in this work were conducted on batches fabricated using a commercial 200 mm epitaxial GaN-on-Si wafer optimized for display applications. Building on the results detailed in this work, as well as findings from previous studies^{23,24} on a non-reported GaN process, future studies could

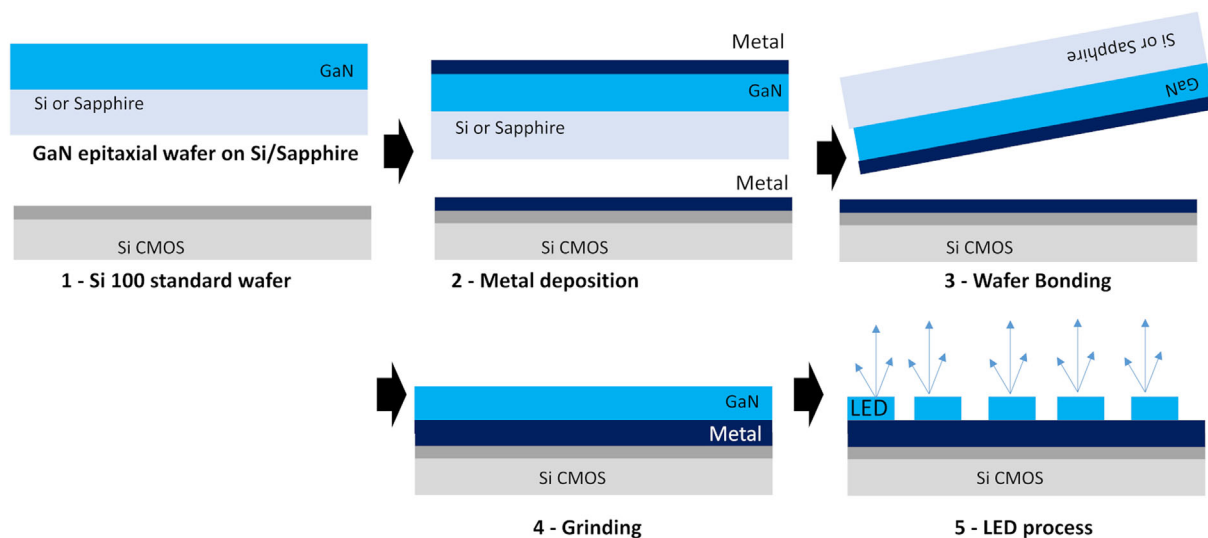


FIGURE 4 Integration process of a 200 mm GaN-on-Si reported on a standard 200 mm Si 100 wafer.

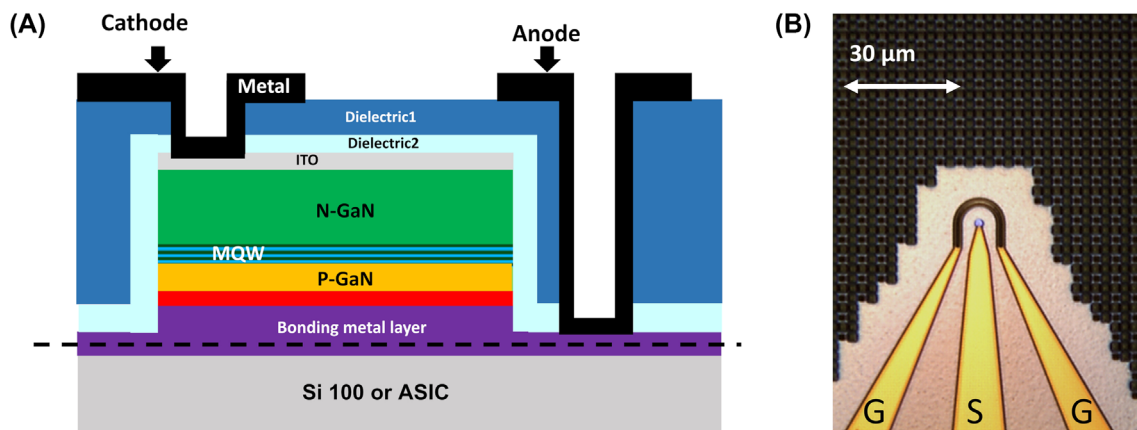


FIGURE 5 (A) GaN microLED on Si 200 mm cross-section; (B) 1.5 μm microLED with GSG (ground-signal-ground) electrical access.

focus on optimizing the GaN-on-Si epitaxial wafer to enable LEDs with higher RF bandwidth. Currently, 200 mm GaN-on-Si epitaxial wafers optimized for data communication are not commercially available today.

4 | MAIN FIGURES OF MERITS

4.1 | Emission: energy efficiency and luminosity

The power consumption per bit of microLEDs is directly proportional to the microLED current density (J_{LED}) and surface of the microLED (S_{LED}), and inversely proportional to the chosen data rate (DR, in bit/s).

$$P(\text{pJ/bit}) = \frac{\text{Electrical power}}{\text{DR}} = \frac{V_{\text{bias}} \cdot J_{\text{LED}} \cdot S_{\text{LED}}}{\text{DR}} \quad (1)$$

Here, we consider a two levels, On-Off Keying (OOK), and modulation. The maximum data rate a microLED can reach is assumed to be the double of optical 3 dB bandwidth. Experimental measurements show that the bandwidth of a microLED increases with current density nearly linearly.²⁴ In order to reach sufficient bandwidth, it is possible to increase current density. However, this requires higher bias voltage, which is in the end limited by electronic circuits and the maximum electric field handled by the device. In Figure 6, the power consumption in pJ/bit is evaluated for three different data rates, in the function of current density, using the experimental IVL of a $9 \mu\text{m}^2$ microLED fabricated. This graph indicates the minimum current density for which the microLED should be able to reach the bandwidth $\text{BW} = 0.5 \cdot \text{DR}$ at a certain energy efficiency target. For instance, to reach an efficiency of 0.1 pJ/bit at a data rate of 1 Gb/s, the microLED should have a bandwidth of

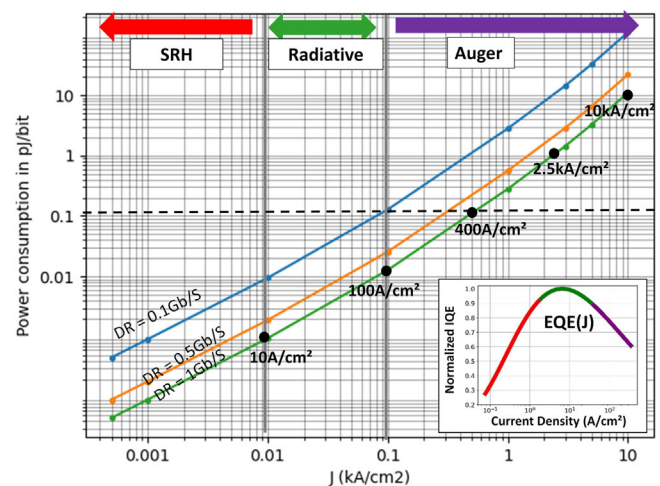


FIGURE 6 Theoretical estimation of energy efficiency in function of current density, for three different data rates, using experimental data of a $9 \mu\text{m}^2$ LED.

500 MHz at a current density of 400 A/cm^2 . Carrier recombination in LEDs is dominated by different mechanisms depending on the current density: Shockley-Read-Hall (SRH), radiative, and Auger recombination. The external quantum efficiency (EQE) as a function of current density, as shown in the inset of Figure 6, can be modeled using the ABC model,²⁵ which indicates which mechanism is dominant depending on the current density. The optimal operating point of a microLED would naturally be at the maximum efficiency. However, it is essential to consider the number of photons per period required to achieve an acceptable Signal-to-Noise Ratio (SNR) and the device bandwidth as a function of current density. This consideration often leads to operating outside the radiative-dominated regime.

The number of photons generated per period (N_p) is proportional to the injected current $I_{\text{LED}} = S_{\text{LED}} \cdot J_{\text{LED}}$

and to EQE, which combines light extraction (LEE) and internal quantum efficiency (IQE). To reach a sufficient SNR number of photons per period must be well above quantum shot noise, approximated as the square root of N_p .

$$N_p = \frac{EQE_{LED}(J_{LED}) \cdot J_{LED} \cdot S_{LED}}{DR \cdot q} \quad (2)$$

Considering these factors of merit, it is clear that both efficiency and RF bandwidth must be optimized to construct a communication link with high power efficiency without degrading the SNR. Once the light is emitted by the microLED, it must be coupled into the optical guide (waveguide or fiber) with minimal loss.

4.2 | Light transmission: coupling microLED to fiber or waveguide

Unlike lasers, microLEDs are spatially and temporally incoherent sources. Coupling such incoherent sources to a waveguide or fiber presents significant challenges due to physical limitations imposed by thermodynamic laws.^{26,27} A substantial portion of the light produced by a microLED will not couple into the fiber or waveguide, regardless of the optical system used, due to the conservation of radiance. Given these constraints, it is worthwhile to explore the coupling of microLEDs into waveguides or fibers and to develop structures that can maximize this coupling efficiency.

4.2.1 | Light transmission through waveguide

In order to build intra-chip optical communication with microLED, coupling a microLED to a waveguide is necessary. Single-mode waveguides are very convenient for transmitting light as they allow a small curvature radius. Waveguides suitable for blue light communication may be built with various material²⁸: GaN, SiN, Al₂O₃, TiO₂. However, as expressed in the introduction of this chapter, coupling light emission from a microLED into a single-mode waveguide (Figure 7) with acceptable loss is challenging, due to the non-coherent nature of light emission. It requires good optimization of the LED stack to enhance lateral emission.

The coupling of microLEDs into waveguides has already been demonstrated, as illustrated in reference (29). In this document, we present a specifically designed structure aimed at optimizing the coupling of a microLED into a GaN waveguide. We conducted 3D FDTD incoherent simulations using ANSYS Lumerical³⁰ to estimate the light transmission from a small source positioned at the focus of a parabolic mirror into a single-mode waveguide (as shown in Figure 7), assuming perfect refractive index matching between the waveguide and GaN. We tested two orientations of dipoles, achieving an average transmission efficiency of 12.5%, with the highest efficiency reaching 20% for one dipole orientation and 5% for the other (illustrated in Figure 8). It is anticipated that this transmission efficiency may decrease as the size of the microLED increases, relative to the size of the

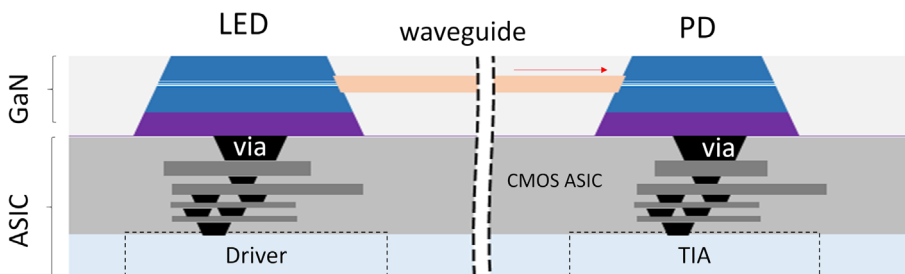


FIGURE 7 MicroLED to microPD transmission with on chip waveguide.

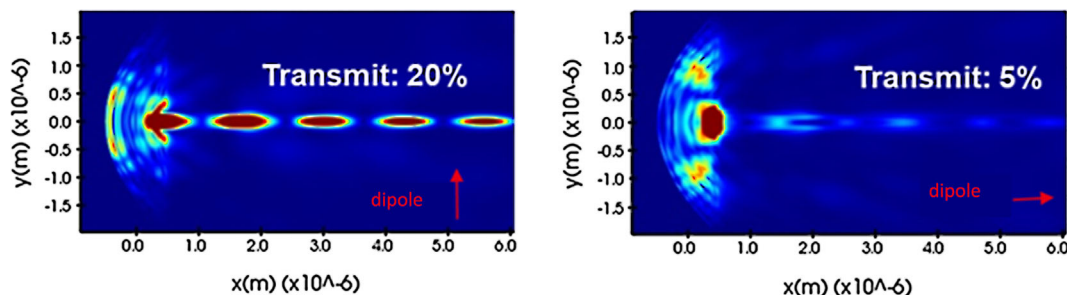


FIGURE 8 Non-coherent 3D FDTD simulation of a microLED coupled to a single-mode waveguide, in the two axes of emission. Average transmission is 12.5%.

parabola. Additionally mirror non-uniformity and loss, or discrepancies between the refractive indices of GaN and the waveguide will decrease this efficiency. These simulations demonstrate the potential for successfully coupling a GaN microLED into a waveguide, highlighting critical design considerations for enhancing device performance.

4.2.2 | Light transmission through a multimode fiber

For chip-to-chip communication on a larger scale, coupling a microLED to a fiber is essential. Multimode fibers can be arranged in a dense configuration with pitches as small as 50 μm . The vertical coupling efficiency between a microLED and a multimode fiber depends on the light's directivity and the Numerical Aperture (NA) of the fiber. MicroLEDs typically exhibit a Lambertian or sub-Lambertian emission pattern, described by $I = I_0 \cdot \cos^n(\theta)$ (Figure 9A). Experimentally, the directivity factor, n , has been measured to be between 2 and 5 when the

microLED is surrounded by a mirror. Fiber bundle makers, such as Lightguide or CeramOptec, propose fiber bundles composed of 50 μm core multimode fibers with NA between 0.22 and 0.37. From microLED emission diagram (Figure 9A), the light coupling efficiency between a microLED and the fiber can be estimated between 4.8% ($n=1$, $\text{NA}=0.22$) and 36% ($n=5$, $\text{NA}=0.37$) (Figure 9B).

4.2.3 | Light transmission through an imaging fiber

Imaging fiber as described in section 1 and presented in Figure 10 contains a very dense arrangement of small diameter fibers, width core diameter below 5 μm . With such imaging fibers, it would theoretically be possible to reach a density of data rate up to 16Tbs/ mm^2 , considering that each core of the fiber is addressed and that each microLED and microPD has a data rate of 1 Gbs. Unfortunately, as fiber core size is scaled down toward single-

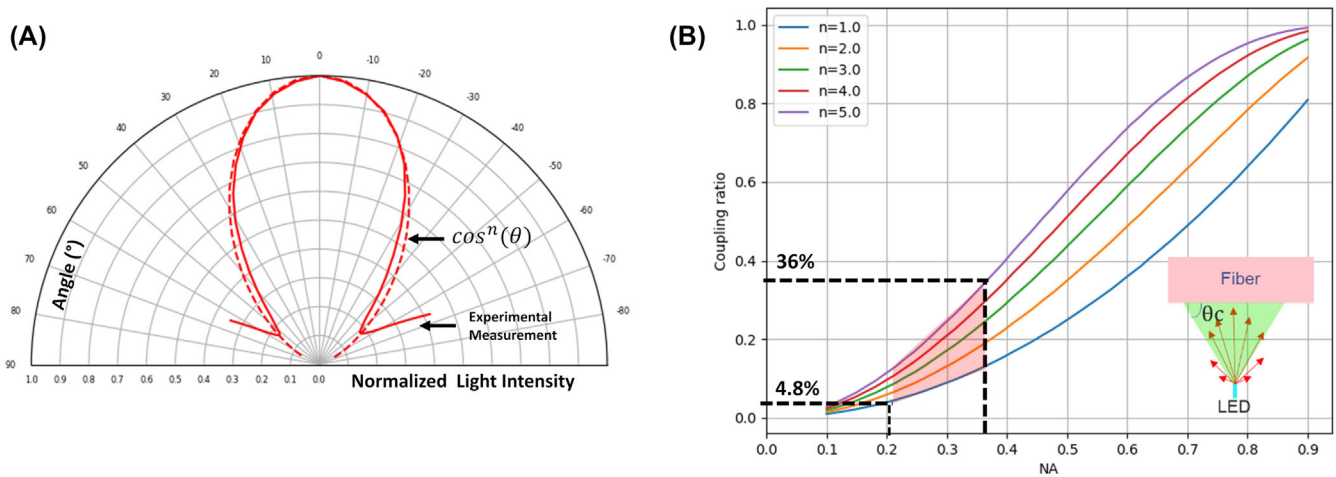
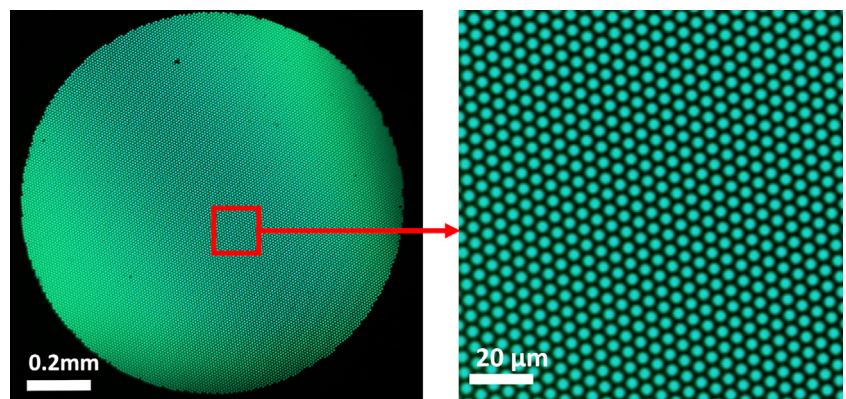


FIGURE 9 (A) Experimental measurement of emission diagram of a 25 μm microLED, fitted to a sub-Lambertian curve with $n = 3.27$; (B) coupling ratio between a fiber and a microLED for different directivity in function of numerical aperture (NA) of the fiber.

FIGURE 10 Sumita leached image bundle (ref 126F0910-7.4) observed through a microscope. The fiber has 16,600 cores, an inner diameter of 1 mm, and an outer diameter of 1.275 mm. Each fiber is arranged in a hexagonal pitch, each core being 4.4 μm .



mode transmission conditions (core size around 3 μm), the light coupling is reduced due to optical mode selection.

Experimentally, the coupling of a matrix of microLEDs and single microLEDs of various sizes has been demonstrated by positioning an imaging fiber close to the emission surface, with a gap estimated to be between 0 and 5 μm , facilitated by a probe positioner (Figure 11). This experiment confirms the feasibility of the approach. However, the coupling efficiency between a single microLED has been experimentally estimated in such conditions to be less than 1%.

To precisely estimate light coupling in one core of the single-mode fiber, we simulate, using ANSYS Lumerical FDTD,³⁰ a simplified version of a GaN microLED with or without a GaN lens on top (Figure 12). Two optical power monitors are needed to extract the total coupling efficiency defined as the fraction of light converted by the quantum well that actually couples into the propagating

mode of the fiber. First, a modal decomposition of the optical power coupled into the fiber is needed to isolate the part coupled in the propagating mode from the evanescent coupling. Then we must place a box calculating the optical flux emitted by the source as it is disturbed by the Purcell effect. The light source is a quantum well traditionally represented by a continuous surface of incoherent electric dipoles. One must compute several independent simulations with a discrete dipolar grid and sum the results to approximate such an incoherent source. Ultimately, that incoherent behavior also means that no symmetry can be used to reduce the simulation size and we are forced to perform expensive 3D FDTD computations.

We have shown that one way to improve the coupling into single-mode transmission fiber is by increasing the directivity (e.g., with a microLens integrated on top of the pixel) or diminishing the pixel size. To further improve

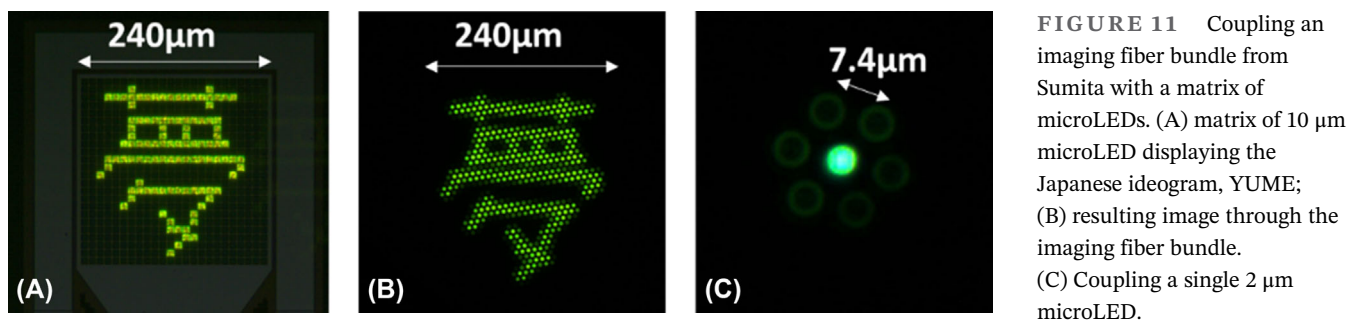


FIGURE 11 Coupling an imaging fiber bundle from Sumita with a matrix of microLEDs. (A) matrix of 10 μm microLED displaying the Japanese ideogram, YUME; (B) resulting image through the imaging fiber bundle. (C) Coupling a single 2 μm microLED.

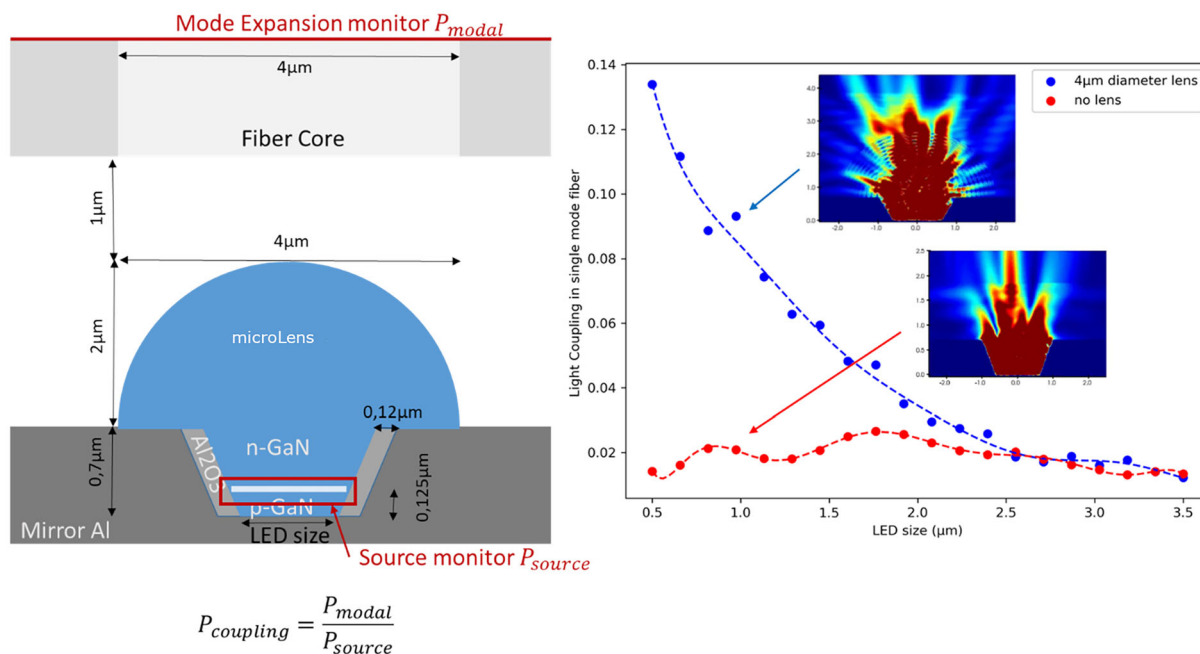


FIGURE 12 FDTD 3D simulations of the light coupling from a microLED in the spontaneous emission regime to a single-mode fiber. More than 50% of the light is reaching the fiber but the optical mode selection is important due to poor emission directivity.

the directivity of emission and thus coupling into the fiber, microLED with a resonant cavity could be particularly beneficial. Besides the challenge of coupling efficiency, a substantial amount of crosstalk between adjacent channels is expected on the emission and reception side, depending on the distance from the microLED to the surface of the fiber, pitch between fiber cores, and flatness of the fiber assembly. These elements are critical in determining the efficiency of emission and reception and must be carefully handled to optimize system performance.

4.3 | Reception efficiency of InGaN/GaN microPD

After discussing the main factors influencing emission and light transmission, we now turn to the final element of the transmission link: the photodiode. In this work, we have considered a microPD made from the same material as the microLED. Photocurrent in the photodiode can be simply expressed as the function of the coupling factor of the microLED into the fiber or waveguide (K), quantum efficiency (QE) of the photodiode, emission EQE , current density, and LED area.

$$iph = K \cdot QE_{PD}(\lambda_{LED}) \cdot EQE_{LED}(J_{LED}) \cdot J_{LED} \cdot S_{LED} \quad (3)$$

The QE of (In)GaN quantum well is strongly wavelength-dependent.³¹ Emission wavelength and maximum reception wavelength are not usually matched in c -plane grown GaN microLEDs, which is called the Stokes shift.³² Indeed, the internal electric field in

c -plane GaN, referred to as the Quantum Confined Stark effect (QCSE) induces a red shift of the emission wavelength. Increasing the current density in the microLED has the opposite effect, which can partially compensate the Stokes Shift in certain conditions of quantum well thickness and material strain.

To better understand the response of a microPD made out of a typical InGaN/GaN LED-epi-structure, we used two different simulation software: Nextnano++³³ to explore the impact of the 1D active region design on incident light absorption properties and ATLAS device simulator by Silvaco³⁴ to perform quasi-3D modeling of the complete device.

The structure we chose to model with Nextnano contains a single InGaN/GaN QW located in the middle of a pin junction. The wavelength dependence of the optical absorption of the single QW is calculated with Fermi's Golden Rule by means of 8-band $k \cdot p$ method after solving the Schrödinger and Poisson equations. We focused on the transitions induced by the transverse electric (TE) mode (parallel to the QW plane). We investigated the evolution of the absorption curve when changing the Indium composition and the thickness of the QW, the reverse bias applied to the pin junction, and the thickness of the depletion region. The simulations confirm some rather intuitive trends: each absorption curve is mainly controlled by the Indium composition and thickness of the QW and the total internal electric field. The absorption coefficient's dependence on wavelength evolves like a staircase pattern controlled by the quantized nature of electron and hole states in the QW as can be seen in the example of Figure 13A. We can confirm

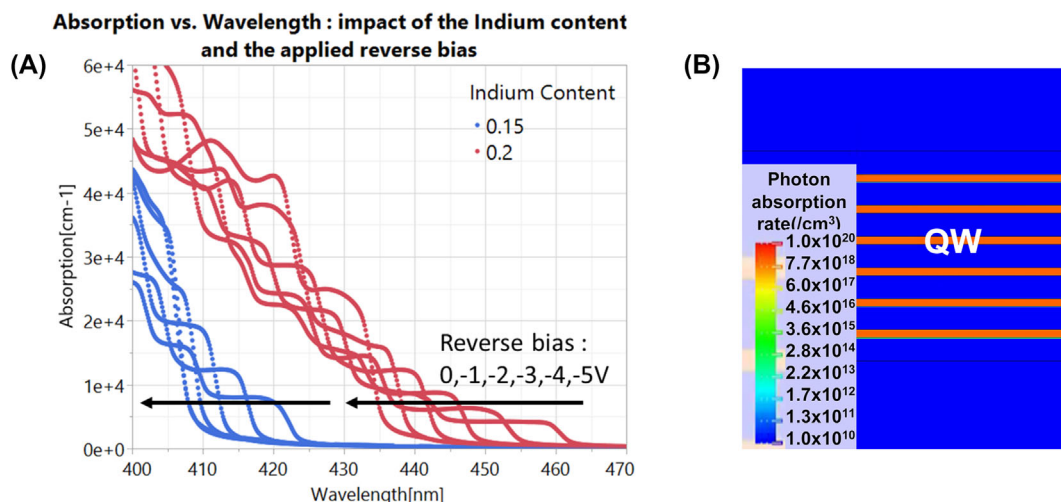


FIGURE 13 (A) Example of the absorption coefficient of a single InGaN QW of 3 nm located in the middle of a GaN pin junction, plotted as a function of the wavelength of the incident light. The blue and red curves correspond to different QW indium compositions and the six curves of each color to the reverse bias applied on the junction: 0, -1, -2, -3, -4, -5 V following the arrow direction. (B) Zoom of the photo-absorption rate in quantum wells simulated by Silvaco at -1 V under illumination at $\lambda = 415$ nm and 10 mW/cm².

that increasing the Indium concentration shifts the absorption to a longer wavelength. We can also explain the blue shift and the rise in amplitude of the first staircase as the reverse bias goes up (0 to -5 V) as the result of compensation of the internal electric field by this applied bias. We decided to use these results as an entry in the TCAD simulations by attributing the right absorption curve to QWs of a given composition and thickness after estimating their internal electric field (Figure 13B).

Quasi-3D TCAD (Technology Computer Aided Design) simulations of a GaN microLED in reception were then performed using the ATLAS device simulator by Silvaco³⁴. We simulated the photocurrent of the microLED biased in reverse voltage (-1 V) and under illumination at different wavelengths from 380 nm to 460 nm.

The simulated structure shown in Figure 14 corresponds to the fabricated microLED structure shown in Figure 5A. In order to save computational time, we defined a half 2D structure with a cylindrical symmetry to model a quasi-3D structure.

Specific models for multi-quantum wells InGaN/GaN devices were implemented such as a three-band wurtzite model based on k.p modeling and a spontaneous and piezoelectric polarization model. Schrödinger equation is

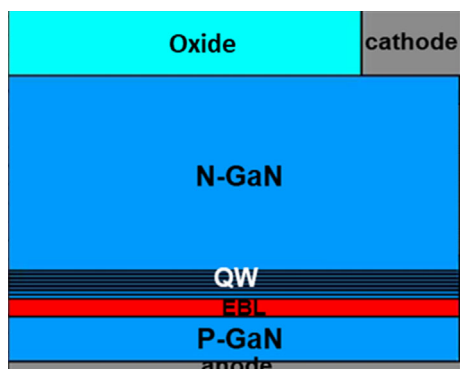


FIGURE 14 2D half cylindrical structure of the simulated GaN photodiode ($L = 50 \mu\text{m}$) used for quasi-3D TCAD simulations.

solved in quantum wells to obtain bound state energies and carriers wave functions. Non-radiative SRH and Auger recombinations were also considered. Modeling of optical cavity effects was performed using the transfer matrix method (TMM) to calculate the interference effects. From the simulated photocurrent we calculated the responsivity of the microPD, which is the ratio of the output photocurrent to the input optical power. Indeed, responsivity is a key metric of photodetector performance.

We studied the impact of the optical cavity on absorption. Figure 15A shows that the interference effects play a major role in the simulated responsivity of the microPD. The interference effects increase the absorption in the structure up to a factor of 3 and generate responsivity peaks at wavelengths that can be tuned by changing the cavity layer thicknesses.

Based on a TEM analysis of the fabricated device, we adjusted the structure layer thicknesses. Then, we tuned the internal polarization and Indium content to modulate the photocurrent as a function of the wavelength to get closer to experimental results. Finally, we observe in Figure 15B that simulated responsivity is in the same order of magnitude as the experimental one. Moreover, the TMM accurately reproduces well the position of the responsivity peak as a function of wavelength.

5 | EXPERIMENTAL PERFORMANCES OF GAN MICROLED AND MICROPD

An experimental setup, as shown in Figure 16 has been developed to perform DC and RF characterization of fabricated microLEDs and microPDs on 200 mm wafers. This includes measurements of current-voltage-luminance (IVL), emission spectrum, spectral responsivity, opto-electrical S-parameters, and transient responses. Additionally, a small signal photoluminescence

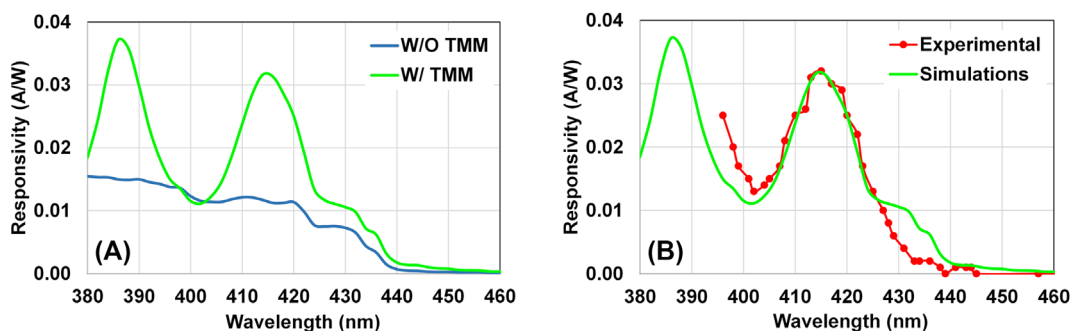


FIGURE 15 (A) Simulation of the responsivity of the microPD with and without the optical cavity effects ($L = 50 \mu\text{m}$, $V = -1 \text{ V}$, $P = 10 \text{ mW/cm}^2$). (B) Experimental and simulated responsivity of the microPD ($L = 50 \mu\text{m}$, $V = -1 \text{ V}$, $P = 10 \text{ mW/cm}^2$).

technique has been implemented to evaluate the epitaxial quality and carrier lifetime within the quantum wells before processing the epitaxial wafers.

The newly developed process enables the fabrication of microLED and microPD devices in a variety of shapes and sizes. A comprehensive mask set has been designed, which includes test structures to model both the RF (radio frequency) and DC (direct current) performances of microPDs and microLEDs ranging in diameter from 1.25 μm to 100 μm . This mask set facilitates a detailed assessment of their performance capabilities for data communication applications. The entire system has been characterized at the wafer level. The microLEDs and microPDs have been fabricated in both matrix configurations (Figure 17) and as individual microLED

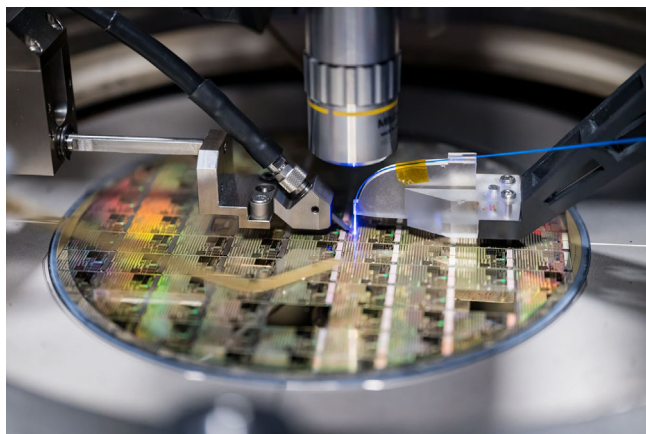


FIGURE 16 A 300 mm probe station showing a 200 mm GaN-on-Si wafer being characterized, using an RF probe and a 200 μm multimode fiber placed above the microLED.

configurations (Figure 5B) featuring RF pad access for enhanced connectivity.

5.1 | Characterization of GaN microLED

To quantify the frequency response of microLEDs, S-parameter measurements were conducted. The experimental setup used is shown in Figure 18. A DC bias is applied to the microLED and a Vector Network Analyzer (VNA) provides small signal modulation. The emitted light was collected by an optical fiber and the signal was transmitted to a high-speed photodiode connected to the second port of the VNA. S-parameters were measured for circular microLEDs with diameters ranging from 3 μm to 100 μm . The bandwidth, extracted from the S21 parameter, was plotted as a function of current density as shown in Figure 19, revealing an almost linear increase in current density across all sizes. Two main factors may limit bandwidth: the recombination lifetime in the wells and the resistance-capacitance (RC) time constant.²⁵ Small signal modeling indicated that recombination lifetime is the limiting factor in the measured samples, identifying it as the primary focus for improvement. The use of GaN on Si(111) epitaxy inherently introduces an internal electric field that separates electron and hole wavefunctions in the wells, thereby increasing the recombination lifetime and limiting bandwidth at low current densities. To mitigate this effect, several approaches are possible. For instance, optimizing the epitaxy structure can reduce this field. Alternatively, using semi-polar or non-polar GaN could be considered, though availability on large substrates remains a challenge. Using S-parameters to

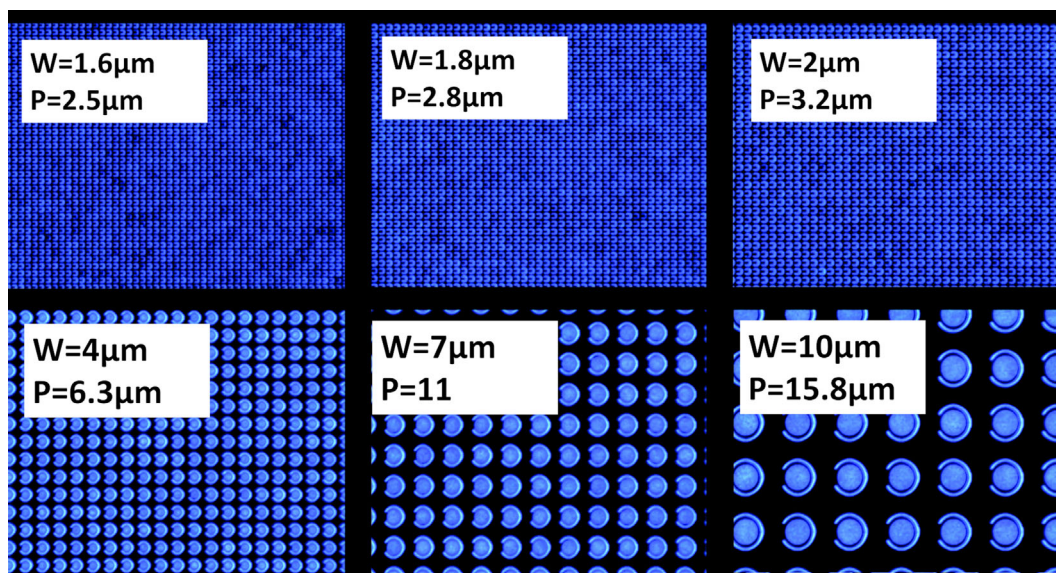


FIGURE 17 Microscope photography of circular blue microLED at various sizes.

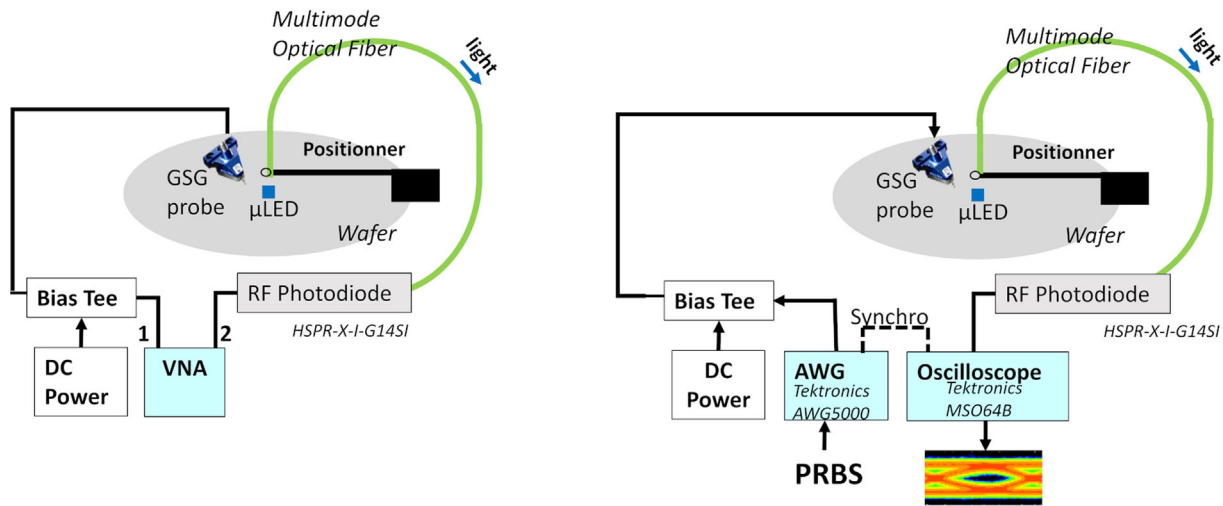


FIGURE 18 Experimental setup used to measure S parameter of microLEDs on the left and eye diagram for an OOK-NRZ emission on the right.

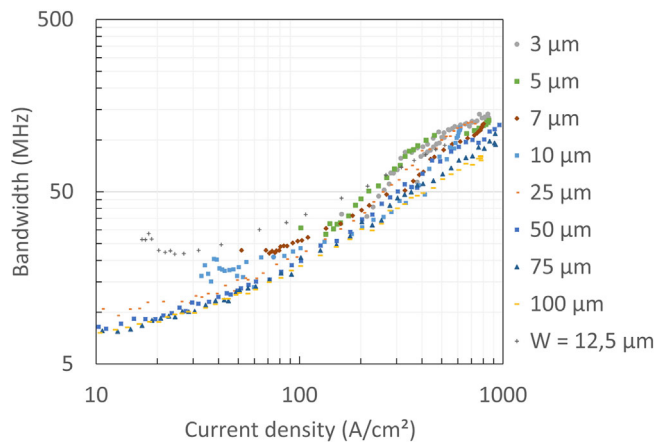


FIGURE 19 Bandwidth as a function of current densities for microLEDs with different diameters ranging from 3 μm to 100 μm and for a square LED with a width of 12,5 μm .

calculate the maximum data rate and IVL measurements, power consumption can be estimated as described in Section 3. For example, a $3 \times 3 \mu\text{m}^2$ microLED operating at a data rate of 600 Mbit/s with a current density of 3 kA/cm^2 has an energy efficiency estimated at 4.5 pJ/bit. To enhance the energy efficiency of the transmission, it is essential to improve the bandwidth of the microLED at low current densities.

Eye diagram measurements were also performed on several microLED sizes at a data rate of up to 1 Gb/s using NRZ OOK (Non-Return to Zero On-Off Keying) modulation, demonstrating open eyes as shown in Figure 20. The best results were obtained with a microLED of 25 μm diameter, which benefited from a better adaptation of the input impedance. Indeed, in experimental bench conditions, all devices under test are

expected to be 50 Ohm adapted. LED fabricated with the process described in Figure 5 have high input resistance R_s due to poor GaN/metal contact quality ($R_s = 1 \text{ k}\Omega$ for a 12.5 μm diameter microLED, $R_s = 250 \text{ Ohm}$ for a 25 μm diameter microLED). Contact resistance scale with device size and is inversely proportional to contact area. Larger devices also benefit from a higher signal-to-noise ratio at the reception side, a consequence of greater optical power. These measurements highlight the critical tradeoff between device optical power, device size, and data rate performance.

5.1.1 | RF characterization of GaN microPD

S-parameter measurements were also performed on the same microLEDs, used as microPDs, by applying a reverse bias. A small signal generated by a Vector Network Analyzer (VNA) was applied to a Thorlabs laser diode, LP405-MF300, emitting at 405 nm. The light output was directed to the microPD through an optical fiber positioned above the device. The modulated photocurrent was measured, amplified by a Transimpedance Amplifier from Femto (HSA-X-1-40) with a gain of 5 kV/A and RF bandwidth of 1.2 GHz, and then fed back to the VNA (Figure 21). In this setup, the maximum bandwidth is limited by the laser diode RF bandwidth, measured at 1GHz. Currently, the absence of blue lasers that can be AC-modulated at GHz frequencies presents a challenge for performing small signal analysis on GaN photodiodes. An alternative solution is to use a pulsed laser. However, small signal measurements offer the advantage of maintaining a constant average optical power, facilitating the extraction of an RF model.

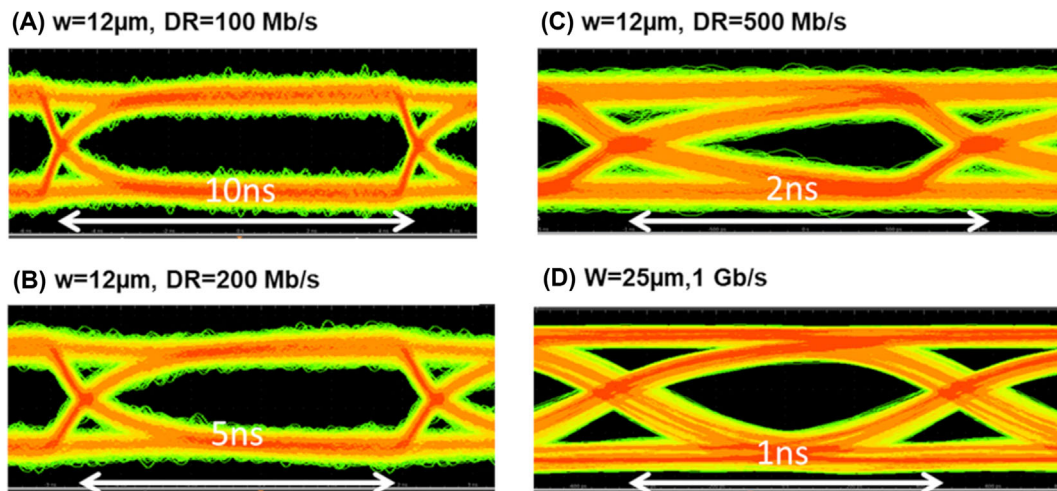


FIGURE 20 Eye diagram measurement with an OOK NRZ modulation using a 700 mV peak-to-peak digital signal generated by an AWG. a, b, and c are eye diagrams measured on a 12 μm width microLED at a current density of 4.4 kA/cm^2 and voltage of 6 V. d) as been measured on a 25 μm diameter microLED at a current density of 500 A/cm^2 at 6 V.

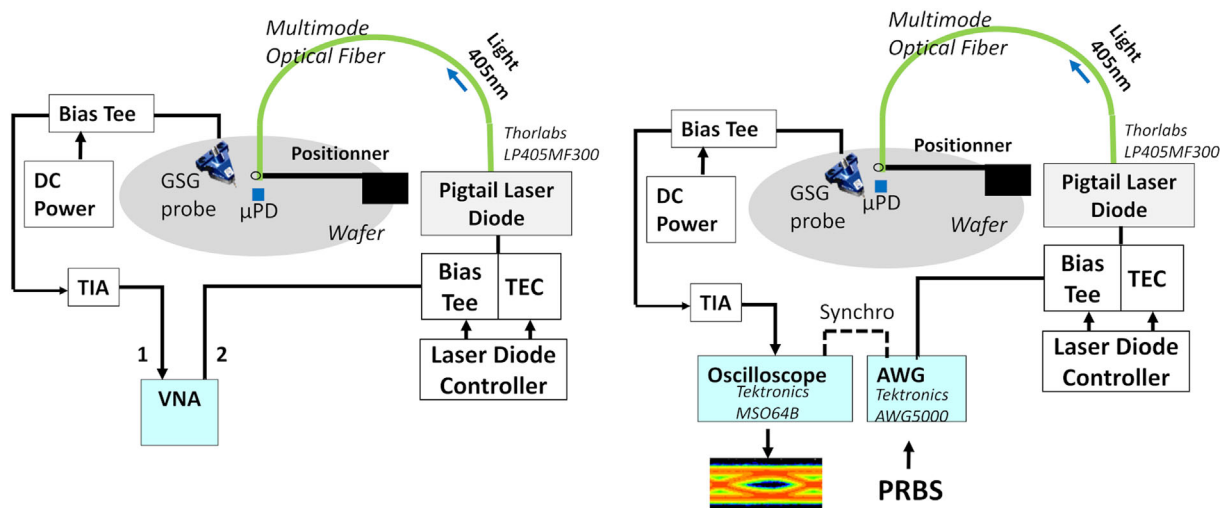


FIGURE 21 Experimental setup used to measure S parameter of microPD on the left and eye diagram for an OOK-NRZ reception on the right.

MicroPDs with diameters ranging from 10 μm to 50 μm were measured, and bandwidth results are shown in Figure 22. The measured bandwidth increased as the size of the microPD decreased, indicating that the main limiting factor is the capacitance of the microPD. Values up to 600 MHz were measured at a reversed bias of 6 V for a 10 μm diameter microPD. An eye diagram of a 36 μm microPD using OOK-NRZ modulation was also measured, showing an eye open at data rates up to 1 Gb/s (Figure 23). These results are promising for the use of such microLEDs as both emitters and receivers in a communication link.

5.2 | Quantum efficiency of GaN microPD

The quantum efficiency of these devices as photodetectors was evaluated using the experimental setup shown in Figure 24. A tunable light source from Zolix connected to a monochromator directs a light signal of a specific wavelength and optical power onto the microPD via an optical fiber coupled with a Thorlabs multimode coupler. The power output from the tunable light source varies with wavelength and requires measurement at each wavelength. Additionally, the wavelength was monitored

using a spectrometer that measures the light wavelength reflected by the multimode coupler. Efficiencies above 20% were achieved at 400 nm, as shown in Figure 24, but the efficiency was negligible at the center wavelength of the emissive spectrum due to the Stokes shift effect. This

highlights the need for a dedicated epitaxial structure for photodiodes. For comparison, the spectral quantum efficiency of two microPDs optimized for green emission at 420 nm was also tested and is presented in Figure 25. A better overlap between the emission spectrum and

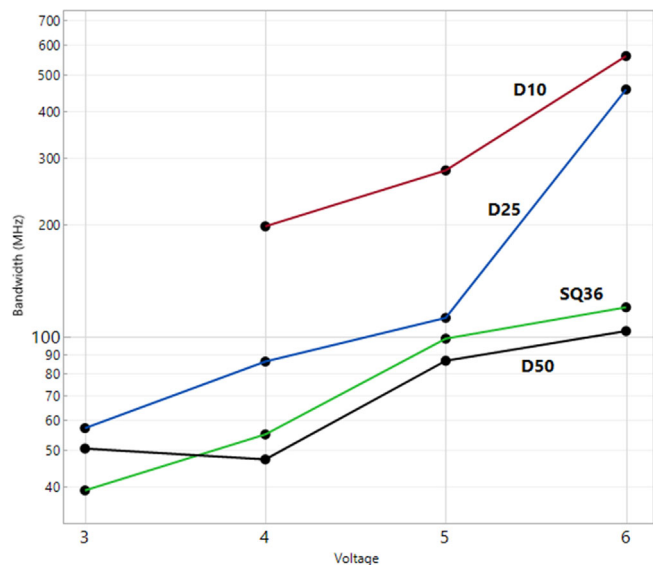


FIGURE 22 Bandwidth of microPD of different size as a function of voltage under a 405 nm laser diode excitation measured on a 200 mm wafer. D10, D25, and D50 are circular microPDs with respective diameters 10 μm, 25 μm, and 50 μm. SQ36 is a square microPD with a 36 μm width.

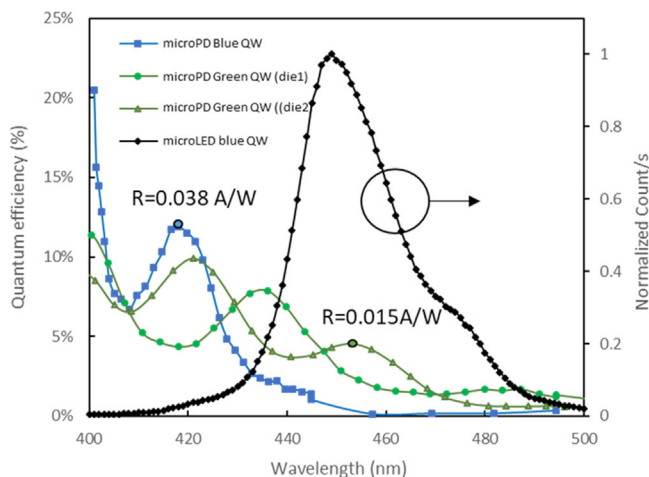


FIGURE 25 Quantum efficiency of a 25 μm diameter GaN microPD at −5,2 V optimized for blue emission as a function of wavelength (blue line). Quantum efficiency of two 25 μm diameter GaN microPDs at −5,2 V optimized for green emission as a function of wavelength (green lines). Typical normalized spectrum for a blue microLED is shown for comparison (black line). The corresponding spectral responsivity R in A/W is also indicated in the graph, with $R = QE \cdot (q \cdot \lambda) / (h \cdot c)$.

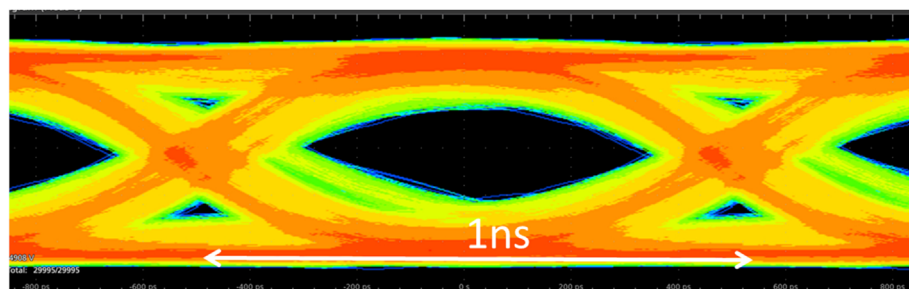


FIGURE 23 OOK NRZ OOK eye diagram reception of a 36 μm (SQ36) microPD at reversed bias of 6 V.

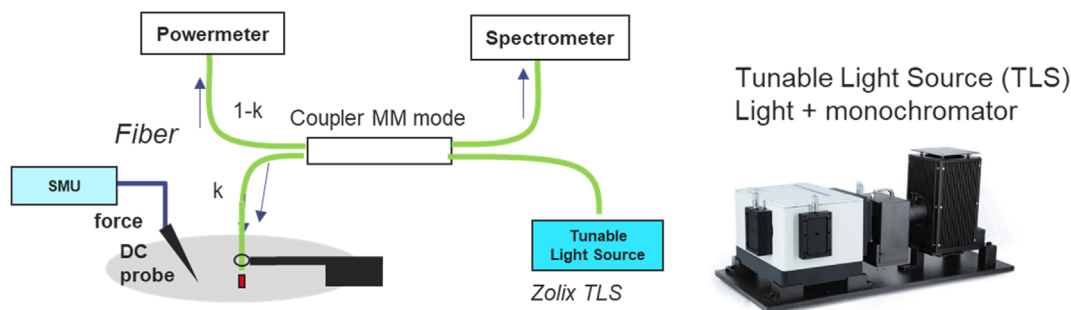


FIGURE 24 Experimental setup used to measure microPD quantum efficiency and responsivity when used as a photodetector b).

spectral quantum efficiency was observed. Moreover, although the two microPDs were fabricated on the same wafer, they showed variations in their efficiency peaks, which can be attributed to differences in the n-GaN thickness affecting the optical cavity height. The optical cavity, which controls the peak of spectral efficiency, must be precisely engineered to ensure that optimum spectral responsivity coincides with the peak emission wavelength.

6 | CONCLUSION

This work introduces the development and evaluation of GaN microLEDs and microPD matrices integrated on 200 mm GaN-on-Si wafers for short-range, high-density optical communications. The research confirms the viability of GaN devices, originally developed for display applications, as effective components for massively parallel and energy-efficient data transmission systems. The integration process, leveraging 200 mm ASIC technology, along with the exploration of various communication system integrations, highlights the potential of these devices to meet the demands of high-performance computing and artificial intelligence applications.

The future of GaN microLED and microPD technology appears promising. On the transmitter side, optimizing the epitaxial wafer design should lead to lower power consumption and higher bandwidth at reduced current densities, significantly improving the energy efficiency of the system toward sub-pJ/bit energy consumption and high data rate density. On the receiver side, tuning the epitaxial stack is essential to maximize quantum efficiency at specific emission wavelengths, thereby optimizing the overall responsiveness of the system. TCAD simulations of InGaN/GaN microPDs, correlated with experimental measurements, show promise for the optimization of these devices. We have explored the coupling of microLEDs through multimode and imaging fibers, and single-mode waveguides using FDTD simulations to understand the limitations of chip-to-chip communication architectures. We point out that while optimizing the design of the devices is beneficial, some optical losses are inevitable as the density of connections increases. The ongoing development of the monolithic integration of microLEDs with ASICs, using hybrid bonding or non-aligned metal-metal bonding as presented in this work, and the industrialization of GaN microLEDs present opportunities to achieve very high data rate densities, potentially revolutionizing the future of short-reach communication by allowing more flexibility in the system architecture of high-power computing systems.

In conclusion, our work provides a solid foundation for future exploration of chip-to-chip communication with microLED and microPD matrices, paving the way for efficient short-range guided visible optical communication using GaN devices.

ACKNOWLEDGMENTS

This work is part of the IPCEI Microelectronics and Connectivity and was supported by the French Public Authorities within the frame of France 2030 and by the Institut Carnot CEA-LETI.

ORCID

Patrick Le Maitre  <https://orcid.org/0009-0007-3191-2546>

REFERENCES

- Zhang Y, Xu R, Kang Q, Zhang X, Zhang ZH. Recent advances on GaN-based micro-LEDs. *Micromachines*. 2023;14(5):991. <https://doi.org/10.3390/mi14050991>
- Kumar V, Kymissis I. MicroLED/LED electro-optical integration techniques for non-display applications. *Appl Phys Rev*. 2023;10(2):021306. <https://doi.org/10.1063/5.0125103>
- Wang K, Song T, Wang Y, Fang C, He J, Nirmalathas A, et al. Evolution of short-range optical wireless communications. *J Light Technol*. 2023;41(4):1019–40. <https://doi.org/10.1109/JLT.2022.3215590>
- Xu H, Davitt KM, Dong W, Song YK, Patterson WR, Nurmikko AV, et al. Integration of a matrix addressable blue/green LED array with multicore imaging fiber for spatio-temporal excitation in endoscopic biomedical applications. *Phys Status Solidi Curr Topics Solid State Phys*. 2008;5(6):2299–302. <https://doi.org/10.1002/pssc.200778716>
- Zhu L, Lai PT, Choi HW. An emissive GaN micro-LED array for visible-light multi-channel communication. 2010 Photon Global Conf PGC 2010. 2010;2–4.
- Pezeshki B, Tselikov A, Danesh C, Kalman R. 8x 2Gb/s LED-based optical link at 420nm for chip-to-chip applications. *IEEE*. 2021;8–10.
- Pezeshki B, Rangarajan S, Tselikov A, Afifi E, Huang I, Pepper J, et al. 304 channel MicroLED based CMOS transceiver IC with aggregate 1 Tbps and sub-pJ per bit capability. *IEEE*. 2024;8–10.
- Park TY, Wang Y, Alkhazragi O, Min JH, Ng TK, Ooi BS. 2-Gb/s ultraviolet-light optical wireless communication by InGaN/GaN multi-quantum well dual-function micro-photodetector. *Appl Phys Lett*. 2024;124(6). <https://doi.org/10.1063/5.0185656>
- Ho KT, Chen R, Liu G, Shen C, Holguin-Lerma J, Al-Saggaf AA, et al. 32 gigabit-per-second visible light communication link with InGaN/GaN MQW micro-photodetector. *Opt Express*. 2018;26(3):3037–45. <https://doi.org/10.1364/OE.26.003037>
- Xu Z, Luo Z, Lin X, Shen C, Wang X, Zhang J, et al. 15.26Gb/s Si-substrate GaN high-speed visible light photodetector with super-lattice structure. *Opt Express*. 2023;31(20):33064. <https://doi.org/10.1364/OE.498632>

11. Memon MH, Yu H, Luo Y, Kang Y, Chen W, Li D, et al. A three-terminal light emitting and detecting diode. *Nature Electron.* 2024;7(4):279–87. <https://doi.org/10.1038/s41928-024-01142-y>
12. Yu H, Xiao S, Memon MH, Luo Y, Wang R, Li D, et al. Dual-functional triangular-shape micro-size light-emitting and detecting diode for on-chip optical communication in the deep ultraviolet band. *Laser Photon Rev.* 2024;2300789(8):1–8. <https://doi.org/10.1002/lpor.202300789>
13. Lin R, Liu X, Zhou G, Qian Z, Cui X, Tian P. InGaN micro-LED array enabled advanced underwater wireless optical communication and underwater charging. *Adv Optical Mater.* 2021;9(12):1–10. <https://doi.org/10.1002/adom.202002211>
14. Yu H, Memon MH, Wang R, Xiao S, Li D, Luo Y, et al. Miniaturized AlGaIn-based deep-ultraviolet light-emitting and detecting diode with superior light-responsive characteristics. *Adv Optical Mater.* 2024;2400499(22):1–8. <https://doi.org/10.1002/adom.202400499>
15. Singh KJ, Huang YM, Ahmed T, Liu AC, Chen SWH, Liou FJ, et al. Micro-LED as a promising candidate for high-speed visible light communication. *Appl Sci.* 2020;10(20):1–32.
16. Margalit N, Xiang C, Bowers SM, Bjorlin A, Blum R, Bowers JE. Perspective on the future of silicon photonics and electronics. *Appl Phys Lett.* 2021;118(22). <https://doi.org/10.1063/5.0050117>
17. Szilagyí L, Khafaji M, Pliva J, Henker R, Ellinger F. 40-Gbit/s 850-nm VCSEL-based full-CMOS optical link with power-data rate adaptivity. *IEEE Photon Technol Lett.* 2018;30(7):611–3. <https://doi.org/10.1109/LPT.2018.2808404>
18. Michard A, Carpentier JF, Michit N, Le Maitre P, Benabes P, Ferreira PM. A sub-pJ/bit, low-ER Mach-Zehnder-based transmitter for chip-to-chip optical interconnects. *IEEE J Select Top Quantum Electron.* 2020;26(2):1–10. <https://doi.org/10.1109/JSTQE.2019.2954705>
19. Templier F. GaN-based emissive microdisplays: a very promising technology for compact, ultra-high brightness display systems. *J Soc Inf Disp.* 2016;24(11):669–75. <https://doi.org/10.1002/jsid.516>
20. Bower CA, Bonafede S, Raymond B, Pearson A, Prevatte C, Weeks T, et al. High-brightness displays made with micro-transfer printed flip-chip microLEDs. *Proc - Electron Components Technol Conf.* 2020;2020-June:175–81.
21. Steudel S, Vertommen J, Boulbar E, Buscemi G, Bach L, Huylenbroeck S, et al. MicroLED display integration on 300mm advanced CMOS platform. *Digest Techn Papers - SID Int Symp.* 2022;53(1):748–51. <https://doi.org/10.1002/sdtp.15598>
22. Quesnel E, Lagrange A, Vigier M, Consonni M, Tournaire M, Le Marchand V, et al. Dimensioning a full color LED microdisplay for augmented reality headset in a very bright environment. *J Soc Inf Disp.* 2021;29(1):3–16. <https://doi.org/10.1002/jsid.884>
23. El Badaoui S, Le Maitre P, Cibié A, Rol F, Litschgi S, Simon J, et al. Impact of GaN μ LEDs aspect ratio on bandwidth and efficiency. In: 2023 photonics north (PN); 2023. p. 1–2.
24. Le Maitre P, El Badaoui S, Cibié A, Simon J, Rol F, Miralles B, et al. GaN μ LED on 200mm silicon wafer toward efficient chip to chip communication. *Solar Energy Light-Emitting Dev.* 2023;SW2D--3.
25. Karpov S. ABC-model for interpretation of internal quantum efficiency and its droop in III-nitride LEDs: a review. *Optical Quantum Electron.* 2015;47(6):1293–303. <https://doi.org/10.1007/s11082-014-0042-9>
26. Riazat UL, Editor A, Stokes LF. Coupling light from incoherent sources to optical waveguides. *IEEE Circ Dev Mag.* 1994; 10(1):46–7. <https://doi.org/10.1109/101.313414>
27. McMahon DH. Efficiency limitations imposed by thermodynamics on optical coupling in fiber-optic data links. *J Opt Soc Am.* 1975;65(12):1479. <https://doi.org/10.1364/JOSA.65.001479>
28. West GN, Loh W, Kharas D, Sorace-Agaskar C, Mehta KK, Sage J, et al. Low-loss integrated photonics for the blue and ultraviolet regime. *APL Photon.* 2019;4(2):026101. <https://doi.org/10.1063/1.5052502>
29. Wang Y, Zhu G, Cai W, Gao X, Yang Y, Yuan J, et al. On-chip photonic system using suspended p-n junction InGaIn/GaN multiple quantum wells device and multiple waveguides. *Appl Phys Lett.* 2016;108(16). <https://doi.org/10.1063/1.4947280>
30. Ansys LI. FDTD: 3D electromagnetic simulator.
31. Kang CH, Liu G, Lee C, Alkhazragi O, Wagstaff JM, Li KH, et al. Semipolar (2021) InGaIn/GaN micro-photodetector for gigabit-per-second visible light communication. *Appl Phys Express.* 2020 Jan;1(1):13. <https://doi.org/10.7567/1882-0786/ab58eb>
32. Zheng R, Taguchi T. Stokes shift in InGaIn epitaxial layers. *Appl Phys Lett.* 2000;77(19):3024–6. <https://doi.org/10.1063/1.1323543>
33. Birner S, Zibold T, Andlauer T, Kubis T, Sabathil M, Trellakis A, et al. Nextnano: general purpose 3-D simulations. *IEEE Trans Electron Dev.* 2007;54(9):2137–42. <https://doi.org/10.1109/TED.2007.902871>
34. Silvaco International, Santa Clara, CA. 2022. Atlas user manual, device simulation software, June 01, 2022, 2022.

AUTHOR BIOGRAPHIES



Patrick Le Maitre was born in Caen, France. He received his engineering degree from Supélec (now CentraleSupélec, France) in 2000, and a Master of Engineering degree from the Tokyo Institute of Technology in 2001. He joined Renesas Technology in 2001 and then moved to NXP Semiconductor in 2004. In 2010, he joined STMicroelectronics in Crolles, focusing on the development of Silicon photonics platforms. Since 2019, he has been a research engineer at the CEA-LETI Institute in France, developing GaN-based emissive devices for microdisplay applications and optical communications.



Anthony Cibié has a Ph.D. degree from Université Grenoble Alpes, France, in 2019, on innovative substrates for GaN-based power devices. In 2020, he joined CEA-LETI to work on GaN-based μ LEDs for display and Visible Light Communication applications.



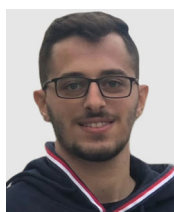
Fabian Rol is a senior scientist at the CEA-LETI Institute in Grenoble, France. He graduated from ESPCI (École Supérieure de Physique et de Chimie Industrielles de la Ville de Paris) and received a master's degree in solid-state physics and condensed matter from the University of Paris-Saclay in 2003. He obtained a PhD in Physics from the University of Grenoble-Alpes in 2007. Since then, he has worked extensively in the field of nitride semiconductor emissive devices and photonic structures, first at UCSB (University of California, Santa Barbara) and Harvard University in the group of Professor Hu until 2010, and later in the industry at CREE, Inc. (now Wolf-speed, Inc.). He joined CEA-LETI in 2019 to work on the development of GaN-based micro-LEDs.



Stéphanie Jacob received the M.Sc. degree in Microelectronics and Telecommunications from Polytech'Marseille, France, in 2004 and the Ph.D degree in microelectronics from the University of Provence, France, in 2008. Her Ph.D work was carried out in CEA-LETI and ATMEL Rousset, France, on the integration, characterization and modelling of silicon nanocrystal memories. In 2008, she joined CEA-LITEN, France, to work on the electrical characterization and modelling of organic transistors and organic photodiodes. Since 2018, she has joined CEA-LETI as a research engineer focusing on the electro-optical characterization and TCAD simulation of GaN LEDs.



Nicolas Michit received his engineering degree from Centrale Nantes in 2016, and his PhD in Silicon Photonics at the Institute of Nanotechnologies of Lyon in 2020. Since 2020, he has been working with CEA LETI Institute as a research engineer, focusing on the optical modeling of GaN-based emissive devices.

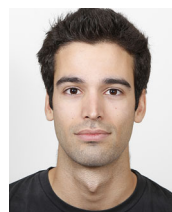


Sultan El Badaoui was born in Tripoli, Lebanon. He received his bachelor's degree in general physics from the Lebanese University in Tripoli, Lebanon, in 2020, and his Master's degree in Nanophysics from Université Grenoble Alpes, Grenoble, France, in 2022. He is currently a PhD student at CEA-LETI and GIPSA-lab in Grenoble, France, working on characterizing and modeling GaN LEDs and

photodiodes for short-reach chip-to-chip optical communication.



Julia Simon, senior scientist in CEA-LETI, graduated in physics from the Polytechnique Institute of Grenoble (INPG) in 1998. She obtained her PhD in solid-state physics in 2001 dealing with optical properties of GaN-based heterostructures grown by MBE. Research engineer in advanced photo-lithography in CEA-LETI from 2001 to 2009, she has gained strong expertise in the area of integration technologies and processes. In 2009, she joined CEA/LITEN, where she took charge of the R&D development of thermoelectrics (20 persons) in a large industrial project until 2014. She moved back to the optical department of LETI, where she is now in charge of the technological integration and device performance of high-resolution μ LED arrays for industrial partners in μ display and optical communication applications.



Bastien Miralles was born in Montpellier, France. He received his engineering degree from Polytech Grenoble in 2018. He joined the CEA-LETI Institute in 2019, working on the integration of GaN μ LEDs.

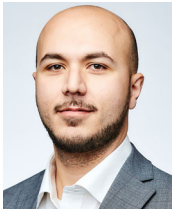


Clément Ballot received his engineering degree in Material Sciences from Grenoble-INP Phelma, located in Grenoble, France, in late 2017. Since 2018, he has been working at the CEA-LETI Institute in France as a research engineer, focusing on the process integration of GaN-based emissive devices for microdisplay applications and optical communications.



Bernard Aventurier was born in Grenoble, France. He received a master's degree from Joseph Fourier University in Grenoble in 1993. He studied and developed new infrared detector technology at the CEA-LETI in Grenoble until 2003 in collaboration with SOFRADIR (now INRED). For the next four years, he worked on the technology of thin-film transistors using low-temperature processes on glass and flexible substrates. During the years 2008 to 2017, he focused his activity on the development of OLED

Display in collaboration with Microoled. Since 2017, he is currently focused on developing process integration for GaN-based micro LED and OLED technologies.



Paolo De Martino joined CEA-LETI, Grenoble France, just after receiving his Master's Degree in Nanotechnologies for ICTs, Politecnico di Torino, in 2020. His research interest spreads from the integration up to the device understanding of LEDs for display applications. He worked both on

phosphorus and III-N-based light-emitting semiconductors for microdisplay and optical communication applications. From 2022, he is also responsible for leading several explorative research projects.

How to cite this article: Le Maitre P, Cibié A, Rol F, Jacob S, Michit N, El Badaoui S, et al. Short range optical communication with GaN-on-Si microLED and microPD matrices. *J Soc Inf Display*. 2024. <https://doi.org/10.1002/jsid.2012>